Numerical Experiments on the Computation of Ground Surface Temperature in an Atmospheric General Circulation Model

CHANDRAKANT M. BHUMRALKAR[1]

The Rand Corporation, Santa Monica, Calif. 90402

(Manuscript received 24 October 1974, in revised form 10 April 1975)

ABSTRACT

The Rand two-level general circulation model has been integrated to compute ground surface (bare land) temperature by solving: 1) the interface heat balance equation without soil heat flux; 2) the interface heat balance equation by including parameterized soil heat flux; and 3) a prognostic equation which includes the heat capacity of the soil as well as an explicit formulation for soil heat flux.

The integrations were performed for 48 hours for the month of January. A comparison of results shows that the most realistic distribution of the ground surface temperature with respect to the amplitude, diurnal range, and the phase relationship between the ground temperature, solar radiation, and soil heat flux is given by the solution of the prognostic equation.

1. Introduction

Meteorologically, the ground surface (as the lower limit of the atmosphere) is an intermediary for the energy exchange between the atmosphere and the underlying surface. One of the important heat sources affecting the atmospheric circulation is the transfer of sensible and latent heat between the surface and the atmosphere. The direction of the energy flow across the interface is primarily determined by the difference between the ground surface temperature and the air temperature immediately above it. Thus in studies of atmospheric circulation it is necessary to know the ground surface temperature accurately.

In more recent meteorological research, the ground surface temperature is usually computed by solving the earth-atmosphere interface heat balance equation under the basic assumptions that the heat capacity of the earth is zero and that there is no *net* heat flux through the air-earth interface. These computations are generally made as a part of more complex atmospheric circulation models—both boundary layer models (Estoque, 1963; Pandolfo *et al.*, 1965; Sasamori, 1970) and general circulation models (GCM's) (Manabe *et al.*, 1965; Gadd and Keers, 1970; Gates *et al.*, 1971; Delsol *et al.*, 1971; Kasahara and Washington, 1971). Recently it has been proposed in some general circulation models (Corby *et al.*, 1972) to compute the ground temperature by solving a prediction equation. Myrup (1969) and Outcalt (1972) have developed a digital surface-climate simulator model to study diurnal surface thermal and energy transfer regimes. Jacobs and Brown (1973) have used a heuristically derived iterative technique to solve the quartic form of the heat balance equation.

Apart from some variations in the formulations of the components of the heat balance equation, the differences in the treatment of the incorporation of soil heat flux in different models for computing the ground surface temperature may be stated as follows:

1) Whereas local atmospheric and soil boundary layer models generally include soil heat flux explicitly, only Delsol *et al.* (1971) have done so in a GCM.

2) Some GCM's (Gates *et al.*, 1971; Manabe *et al.*, 1965) neglect the soil heat flux, while others (Kasahara and Washington, 1971; Gadd and Keers, 1970) include it in a parameterized form. However in both of the above instances, the soil heat capacity is assumed to be zero.

3) The GCM using a prognostic equation to compute ground surface temperature (Corby *et al.*, 1972) neglects the conduction from below but considers a non-zero heat capacity for the soil.

The purpose of this paper is to examine the computation of ground surface temperature in an atmospheric general circulation model with specific reference to the inclusion of soil heat flux. We plan to use the existing version of Rand's two-level GCM to compute the ground temperature by using different formulations of soil heat flux, and by solving a prognostic equation for the ground temperature. We propose to compare the results to determine the most realistic method for the computation of the ground *surface* temperatures in a GCM.

[1] Current affiliation: Stanford Research Institute, Menlo Park, Calif. 94025.

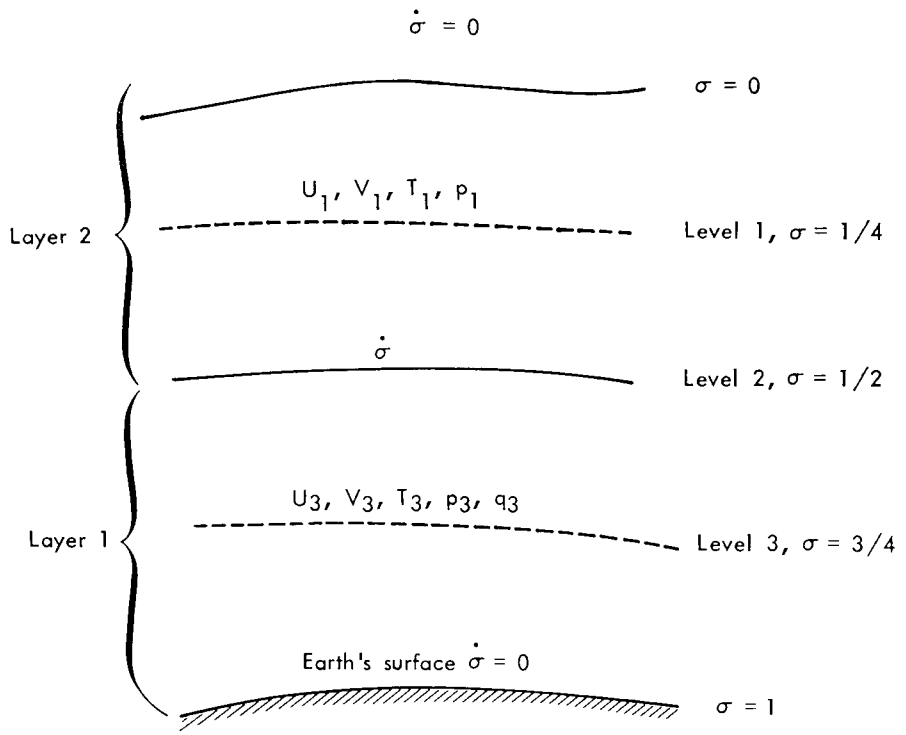

FIG. 1. Schematic vertical representation of the model.

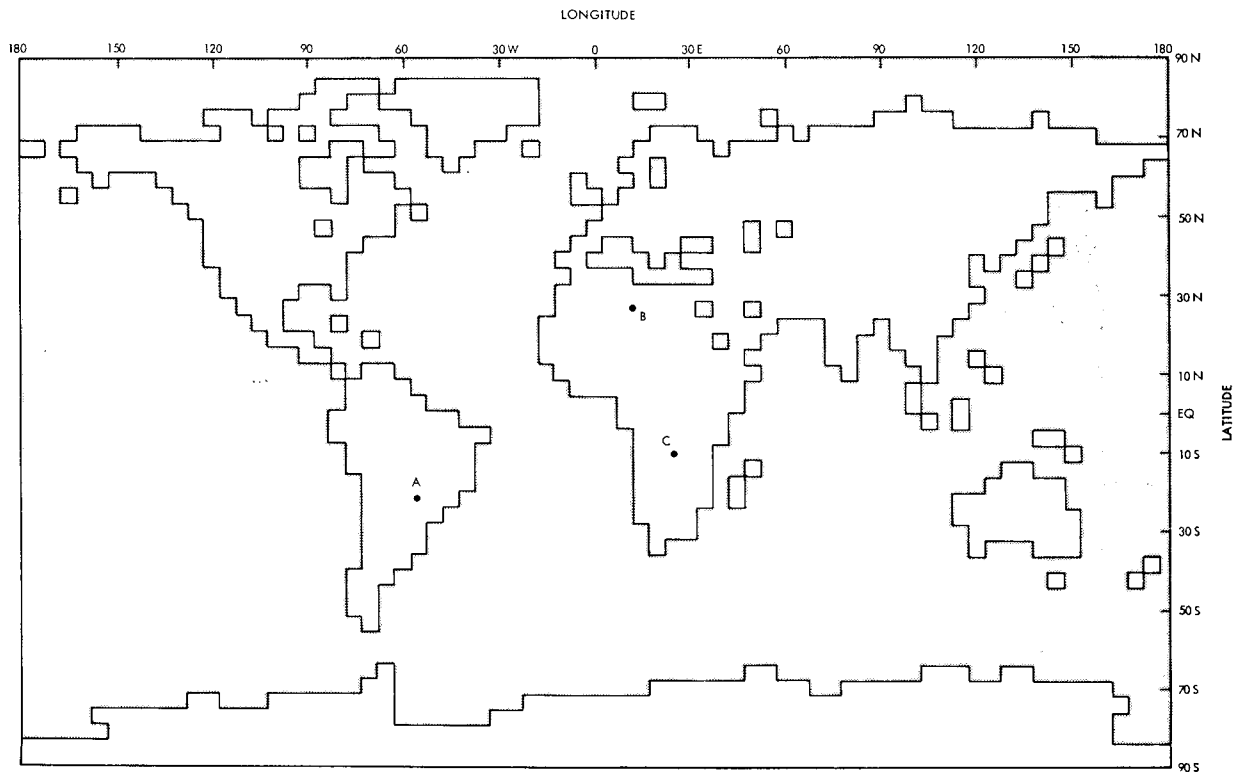

FIG. 2. Land areas as resolved by the model and the locations of selected points A, B and C.

2. Basic circulation model

The basic model equations used in this study are those described in a comprehensive description and documentation of a two-level atmospheric general circulation model by Gates *et al.* (1971). Fig. 1 shows a schematic cross section of the two-layer model. The model equations are set in the so-called σ coordinate system in which the earth's surface is always the coordinate surface $\sigma=1$. Here σ is the dimensionless vertical coordinate, $0\leqslant\sigma\leqslant 1$, increasing downward, and is given by $\sigma=(p-p_t)/(p_s-p_t)$, where p is the pressure, p_t is the (constant) tropopause pressure, and p_s is the (variable) surface pressure. The grid spacing in the horizontal is 4° latitude and 5° longitude. The time integration proceeds in steps of 6 min and the forcing terms of the governing equations are computed every half-hour (i.e., every fifth time step). Fig. 2 shows the land areas of the globe as resolved by the model as well as three selected locations, A, B and C. The ground surface temperature is computed by solving the heat balance equation at the air-ground interface; over oceans the sea surface temperature is prescribed to be constant throughout the integration.

3. Solution of the heat balance equation without soil heat flux: The control experiment

In order to determine the effect of soil heat flux on ground surface temperature calculations, we integrated the basic circulation model *without* including the soil heat flux in the heat balance equation. Thus, for the control experiment, we computed the ground surface temperature by solving the heat balance equation

$$R+H+LE-S=0 \tag{1}$$

at the earth-atmosphere interface. Here R is the net longwave radiation emitted from the surface; H and LE are, respectively, the sensible and latent heat fluxes from the surface; and S is the total solar radiation absorbed by the ground. All the components are expressed in SI units. As described by Gates *et al.* (1971), the heat flux components (except for S) depend upon ground temperature, which is computed from Eq. (1) by backward implicit method. In this study, since there is more emphasis on comparison between different experiments rather than actual results of any one, we have used *exactly the same* formulations for H and LE as in Gates *et al.* (1971). Thus substituting for R, H and LE in (1) and rearranging, we obtain the following expression for computing the ground temperature at time $t+\Delta t$:

$$T_g^{t+\Delta t}=\frac{S-R+C_HT_4+\dfrac{LC_H}{C_p}\left\{q_4+\mathrm{GW}\left[\dfrac{dq_s(T_g)}{dT}T_g-q_s(T_g)\right]\right\}}{C_H\left[1+\dfrac{L}{C_p}\mathrm{GW}\dfrac{dq_s(T_g)}{dT}\right]} \tag{2}$$

(omitting the superscript t from terms on the right-hand side).

Here

$$C_H=\rho_4C_DC_p|\mathbf{V}_s|,$$

where:

- ρ_4 density of air at anemometer level (level 4)
- C_D surface drag coefficient
- C_p specific heat of air at constant pressure
- $|\mathbf{V}_s|$ measure of surface wind speed
- T_g (on right-hand side) ground surface temperature at time t
- T_4 air temperature at anemometer level
- L latent heat of evaporation
- q_s, q_4 mixing ratios at the surface and anemometer level
- GW dimensionless measure of ground wetness taking values from 0 (for dry conditions) to 1 (for completely wet conditions).

The sign convention preceding the symbols in (1) is chosen so that the terms are positive when the flux is away from the ground and negative when it is toward the surface. It may be remarked here that anemometer level is not an explicit level of the model and the quantities there are not predicted, but are obtained from the predicted variables at levels 1 and 3.

With initial and boundary conditions appropriate to January, the GCM was integrated for 48 hours.

a. *Magnitude of maximum ground surface temperature*

Fig. 3 shows the global distribution of daily maximum surface temperature as simulated by the GCM for the month of January. Though there are very few records of maximum surface temperature for natural surfaces, there is no evidence to indicate that the distribution of ground surface temperature in continental areas south of 30°N is realistic. Specifically in the Sahara region, the isotherms are more typical of late spring or early summer rather than January (Geiger, 1965). Similarly the values of 90°C or more in equatorial west Africa, which is wet and forested region, appear to be too high. Since the actual value of maximum surface temperature

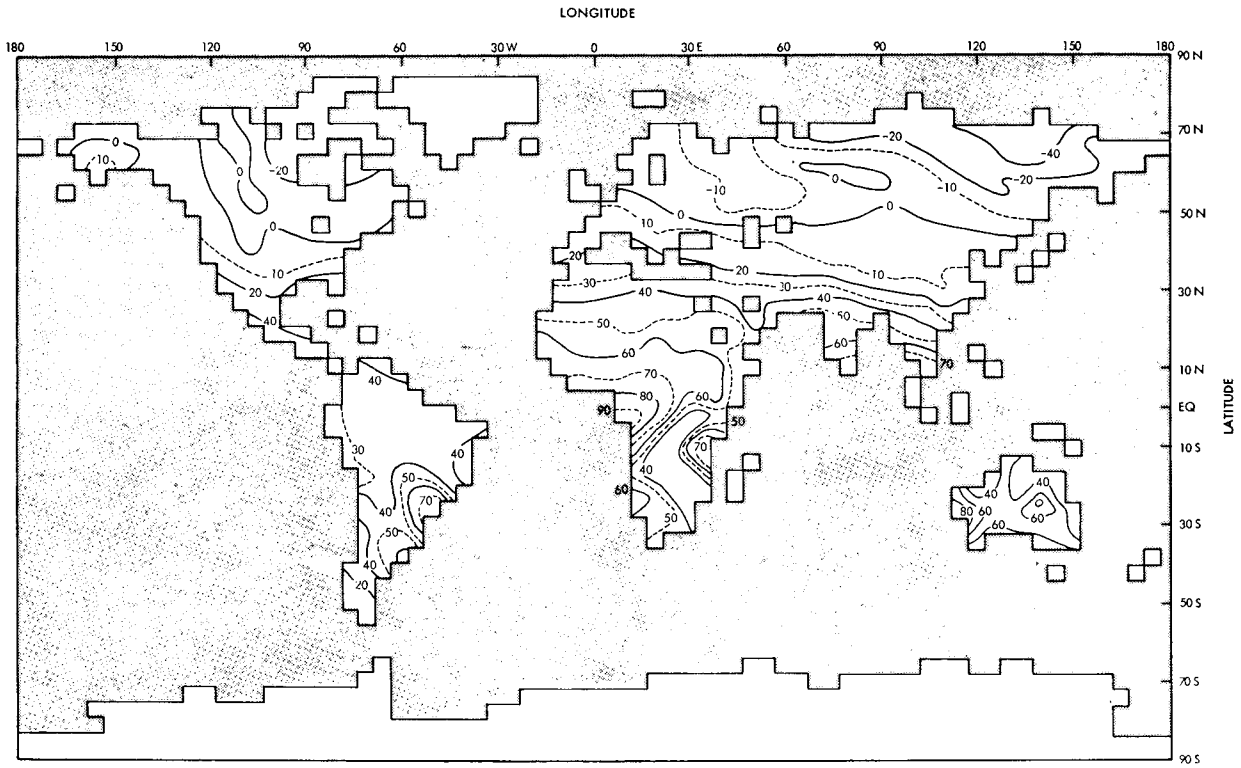

FIG. 3. Daily maximum ground surface temperature (°C): Control Experiment (January).

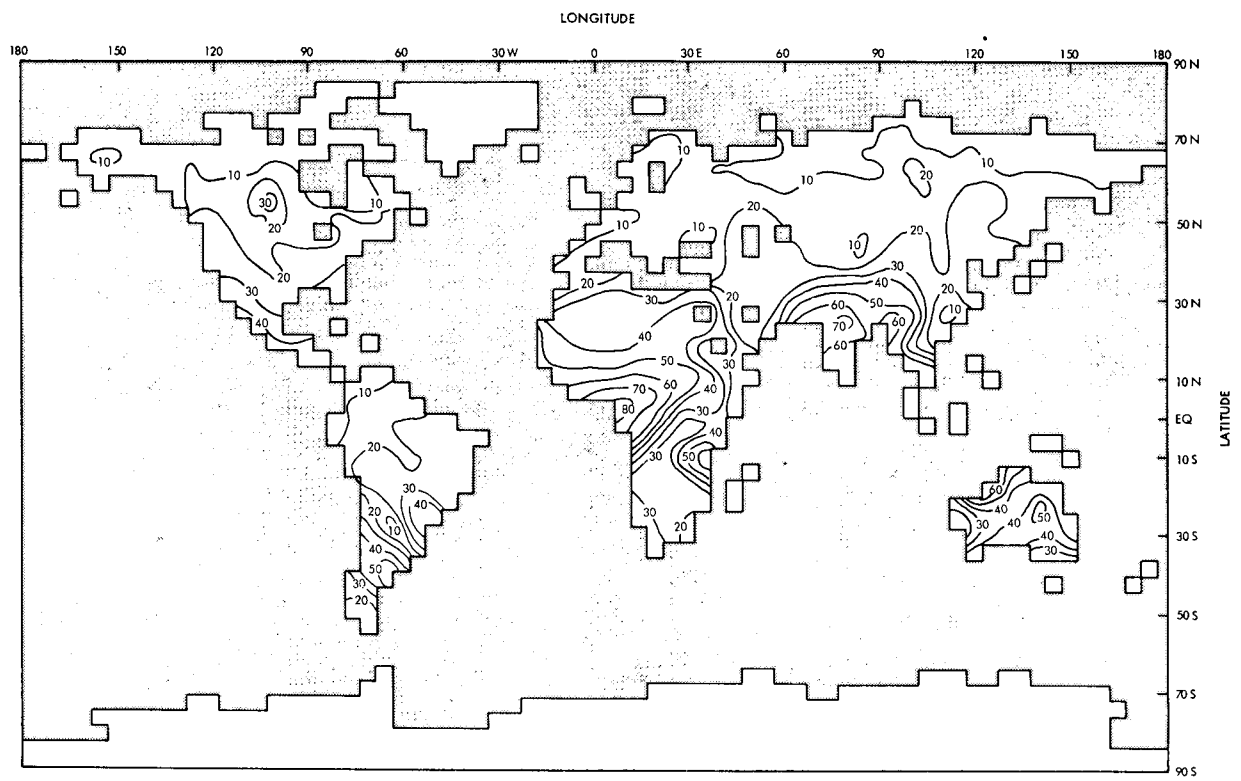

FIG. 4. Diurnal range of ground surface temperature (°C): Control Experiment (January).

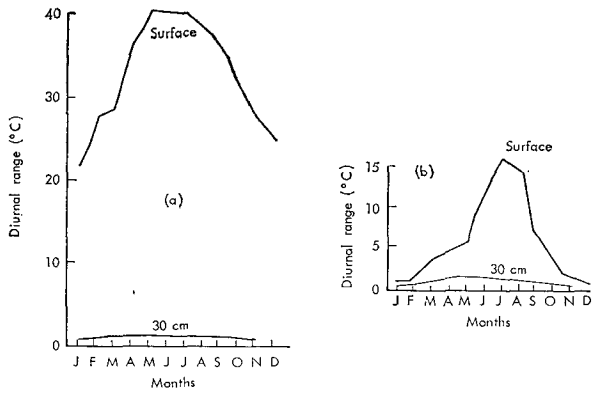

FIG. 5. Annual course of diurnal range in soil temperature at (a) Ginza, Egypt, and (b) Zurich, Switzerland (from Chang, 1958).

depends not only on the radiation, evaporation and heat transfer in air but also on the heat transfer into the soil, and we have not incorporated this in Eq. (1), it seems likely that this exclusion is largely responsible for the unrealistic distribution of ground surface temperature in the control experiment.

b. Diurnal range of ground surface temperature

Fig. 4 shows the global distribution of the diurnal range of the surface temperature obtained in the control experiment. In nature the amplitude of the surface diurnal variation changes considerably, particularly with the time of the year. In winter, the daily temperature oscillation at the surface is much smaller than in summer (Fig. 5). In general, outside the tropics, for clear days and bare surface, 25°C is a fairly representative value of diurnal oscillation in summer (Sutton, 1953). In winter this value is about 2 or 3°C. It can be seen from Fig. 4 that the diurnal oscillation values for the control experiment are rather unrealistic, exceeding 50°C in part of South America. Also, within summer tropical regions, observations (Sinclair, 1922) have shown a diurnal range of 56°C *in the extreme*, whereas the control experiment shows a diurnal range in excess of 70°C over wide areas of tropical regions, even in the winter hemisphere.

c. The time of maximum surface temperature

The time of maximum surface temperature is also of considerable interest in analysis of heat transfer in the atmosphere. Observations have shown that on clear days the surface attains its maximum temperature about 1 hour after the time of maximum solar radiation (Lonnquist, 1962; Sutton, 1953, p. 197). It may be mentioned here that this lag of the daily maximum temperature increases with depth in the soil. Fig. 6 shows a plot of computed ground temperature and solar radiation as a function of local time at two selected locations (A and B, Fig. 2) of the grid. It is seen that there is *no* time lag between solar radiation and maximum ground temperature. This result also follows from the analytical solutions and is to be expected when heat capacity is neglected.

In summary, the results of the control experiment show that:

1) The daily maximum surface temperature is too high, especially in equatorial and tropical regions of both the summer and winter hemispheres.

2) The amplitude of the diurnal temperature oscillation is unrealistic in these same regions.

3) There is no time lag between the maximum solar radiation and the maximum ground surface temperature.

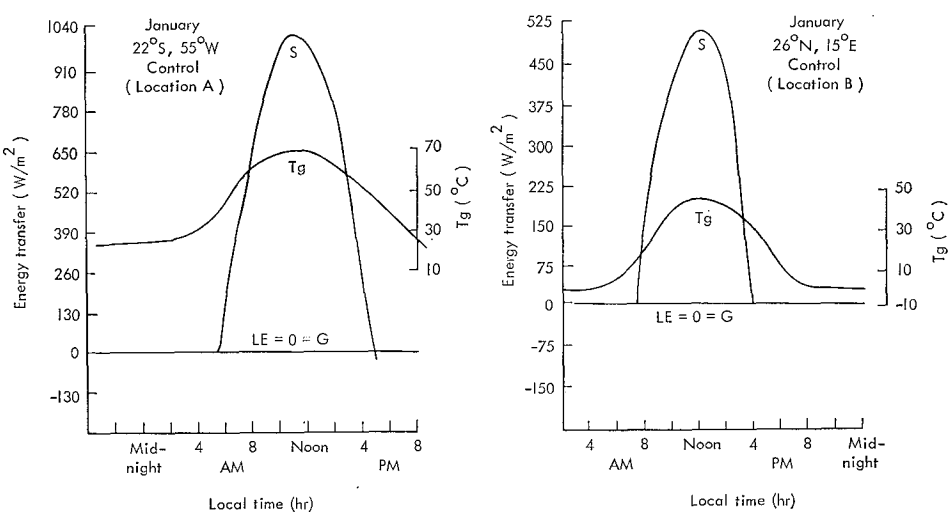

FIG. 6. Daily variation of ground surface temperature (°C) and solar radiation (W m^{-2}) at two selected locations: Control Experiment (January).

TABLE 1. Formulations of soil heat flux G used in Eq. (3).

Experiment	Formula for soil heat flux G	Source
Control	$G=0$	Gates *et al.* (1971)
1	$G=\frac{\lambda}{D}(T_g-T_D)$	Estoque (1963), (L); Pandolfo *et al.* (1965), (L); Myrup (1969), (L); Delsol *et al.* (1971), (GCM); Sasamori (1970), (L)
2	$G=\mu R_N$	Gadd and Keers (1970), (GCM)
3	$G=0.3H$ and $LE=H$	Kasahara and Washington (1971), (GCM)

Note: In source column, L=local atmospheric and soil boundary layer models; GCM=atmospheric general circulation models.

4. Solution of heat balance equation including soil heat flux: Experiments 1 to 3

In the previous section we have discussed the computation of the ground surface temperature as calculated in the control experiment with the Rand two-level atmospheric circulation model. In this section we describe the results of three numerical experiments which were performed to determine the effect of incorporating the soil heat flux at the surface on the ground surface temperature. In these experiments the ground surface temperature was obtained as a solution of the generalized interface heat balance equation

$$R+H+LE+G-S=0, \tag{3}$$

where R, H, LE and S have the same meaning and formulations as in the control experiment [Eq. (1)], and G is the soil heat flux at the surface. Eq. (3) was solved for *bare* land points only. Table 1 shows the formulation of G used in the three experiments.

a. *Experiment 1*

In this experiment, Eq. (3) was solved by approximating the soil heat flux G by the formula

$$G=\frac{\lambda}{D}(T_g-T_D), \tag{4}$$

where λ is the thermal conductivity, D is the damping depth of diurnal temperature oscillations, T_g is the ground surface temperature and T_D is the soil temperature at depth D.

Following de Vries (1963), we specified λ as a function of the surface moisture as represented by the ground wetness parameter GW in the Rand GCM. Thus λ (units: W m^{-1} K^{-1}) varied from a value of 0.5 for dry soil (GW=0) to 2.5 for GW$\geq$0.2, the variation being assumed linear for 0<GW<0.2; these values correspond closely to those given by Priestley (1959). The damping depth D also depends upon the moisture content of the soil such that it is nearest to the surface in a dry and completely wet soil and goes much deeper in a moderately wet soil (Chang, 1958). In experiment 1, we specified D to vary with ground wetness such that it increased linearly from 0.1 to 0.5 m as GW increased from 0 to 0.5 and decreased linearly from 0.5 to 0.1 m as GW increased from 0.5 to 1.0. The maximum value of 0.5 m was chosen on the basis of observations which show that for common soils the diurnal temperature wave does not penetrate below 0.5 m (de Vries, 1963). T_D was specified to be 280 K at all the bare land grid points.

Substituting Eq. (4) in Eq. (3) and following the same procedure as in the control experiment, we obtain the equation

$$T_g^{t+\Delta t}=\frac{S-R+C_HT_4+\frac{LC_H}{C_p}\left\{q_4+\mathrm{GW}\left[\frac{dq_s(T_g)}{dT}T_g-q_s(T_g)\right]\right\}+\frac{\lambda}{D}T_D}{C_H\left[1+\frac{L}{C_p}\mathrm{GW}\frac{dq_s(T_g)}{dT}\right]+\frac{\lambda}{D}}. \tag{5}$$

It may be noted that Eq. (5) is similar to Eq. (2) except for additional terms in the numerator ($\lambda T_D/D$) and the denominator (λ/D) which arise from the inclusion of the soil heat flux in Eq. (3).

A comparison of global distribution of ground surface temperature (not shown) obtained in Experiment 1 with that of the control experiment shows a general decrease of 20°C in the amplitude both of the ground surface temperature as well as the diurnal range. Fig. 7 shows the comparison at three selected locations. It can be seen that the inclusion of soil heat flux G in the heat balance equation has decreased the amplitude of ground surface temperature at locations A and B appreciably. However, at location C this apparently had no effect on the ground temperature. The reason for these differences

TABLE 2. Ratio of LE, H and G to net radiation R_N at selected locations A, B and C.

Experiment	Locations A and B			Location C		
	LE/R_N	H/R_N	G/R_N	LE/R_N	H/R_N	G/R_N
Control	~0	1	0	1	~0	0
1	~0	0.6	0.4	0.9	~0	0.1

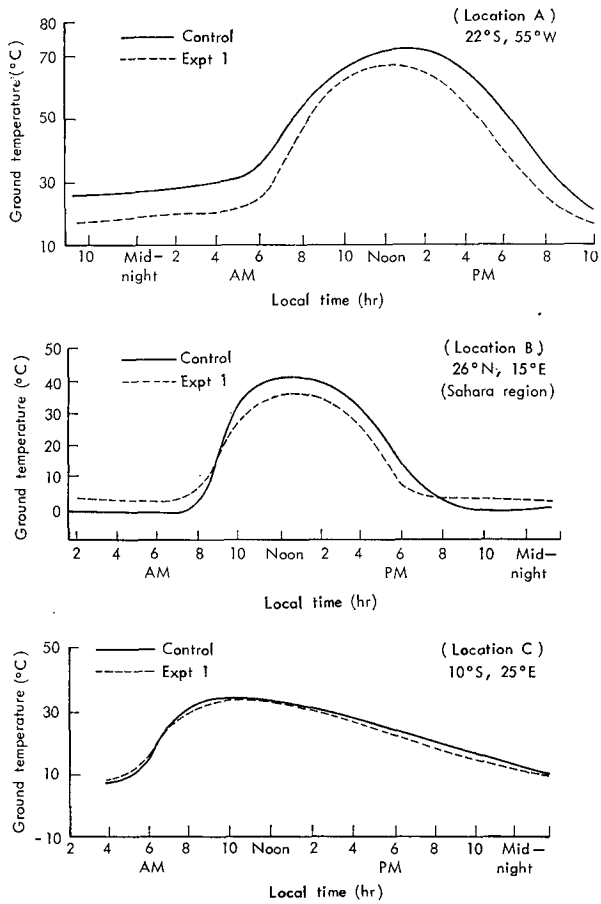

FIG. 7. Comparison of daily variation of ground surface temperature (°C) between Control Experiment and Experiment 1 at three selected locations (January).

can be attributed to very dry surface conditions (GW∼0) at locations A and B but almost wet conditions (GW∼0.9) at location C. Table 2 shows the values of heat balance components LE, H and G relative to the net radiation R_N at locations A, B and C for both the control experiment and Experiment 1.

This shows that while heat flux into the ground is important for dry conditions (∼40% of R_N for bare ground), it is not very significant (∼10% of R_N) in affecting ground temperatures for very wet conditions. These results compare well with observations (Sellers, 1965). Just as in the case of the control run, Experiment 1 also does not show a time lag between maximum solar radiation and maximum ground temperature (Fig. 8). Similarly, it may be noted that there is no time lag between maximum soil heat flux and maximum ground temperature. These results are at variance with conditions in nature, which show that the maximum surface temperature occurs 3 hours *after* a maximum in soil heat flux (Johnson, 1954).

Thus in summary, Experiment 1 shows that while the inclusion of soil heat flux in the heat balance equation gives relatively lower values of ground surface temperature, the relationship of ground temperature with solar radiation and soil heat flux is not realistic. The most important drawback of the formulation of G used in this experiment is the specification of the same constant value for T_D at all the bare land points on the globe. Moreover, the damping depth D, which can vary considerably over the globe, also has to be specified.

b. *Experiment 2*

Gadd and Keers (1970) have expressed the heat flux (G) into the ground as a fraction of net radiation (R_N) at the surface so that

$$\frac{G}{R_N}=\mu, \tag{6}$$

where $R_N=(S-R)$; and μ is assigned a value of 0.1 for

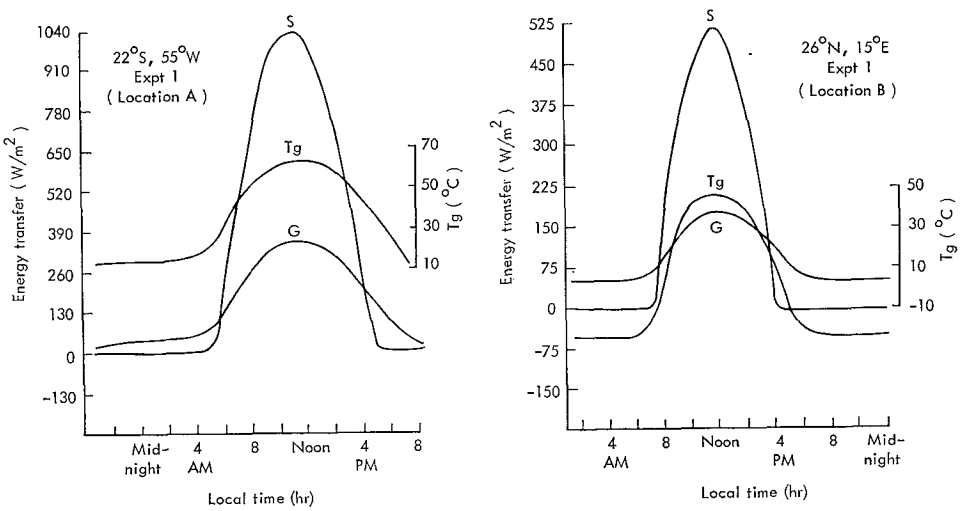

FIG. 8. Daily variation of ground surface temperature (°C), solar radiation (W m^{-2}) and soil heat flux (W m^{-2}) at two selected locations: Experiment 1 (January).

$R_N \geqslant 0$ (daytime) and 0.5 for $R_N < 0$ (nighttime). Thus, for Experiment 2 we obtain the ground temperature as a solution of the equation

$$H+LE-(1-\mu)R_N=0. \tag{7}$$

[This is obtained by substituting $G=\mu R_N$ in Eq. (3).]

An expression for computing the ground temperature T_g [corresponding to Eq. (5) of Experiment 1] is thus given by

$$T_g^{t+\Delta t}=\frac{(1-\mu)R_N+C_HT_4+\frac{LC_H}{C_p}\left\{q_4+\mathrm{GW}\left[\frac{dq_s(T_g)}{dT}T_g-q_s(T_g)\right]\right\}}{C_H\left[1+\frac{L}{C_p}\mathrm{GW}\frac{dq_s(T_g)}{dT}\right]}. \tag{8}$$

The results (Fig. 9) indicate a rather insignificant decrease in the daytime magnitude of surface temperature as compared to that of the control experiment. However, during nighttime the surface temperatures of Experiment 2 were considerably higher than those of the control experiment. These features can be attributed to two different values of μ used in Eq. (2): lower for daytime and higher for nighttime. The values of diurnal range were also affected only to the extent that the minimum in Experiment 2 was higher than that in the control experiment. In this case also there is no phase lag between the ground surface temperature, solar radiation and the soil heat flux. It may be mentioned here that Gadd and Keers (1970) did not compute LE and H explicitly, as we did in Experiment 2. They obtained the latent and sensible heat fluxes by partitioning the available flux (R_N-G) at the surface.

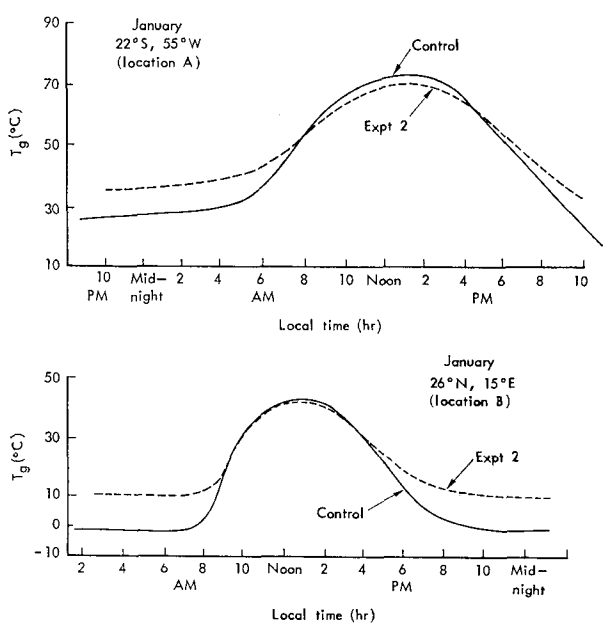

FIG. 9. Comparison of daily variation of ground surface temperature (°C) between Control Experiment and Experiment 2 at two selected locations.

c. Experiment 3

In their general circulation model, Kasahara and Washington (1971) computed the ground surface temperature over land by solving Eq. (3). On the basis of a study by Sasamori (1970), they prescribed the soil heat flux G to be a fraction of sensible heat flux H; also they specified a value of *unity* to the Bowen ratio (H/LE). Thus, if we substitute

$$\left.\begin{aligned} G&=0.3H \\ LE&=H \end{aligned}\right\}, \tag{9}$$

Eq. (3) becomes

$$R-S+2.3H=0,$$

or substituting for H in terms of ground temperature T_g, we obtain

$$T_g^{t+\Delta t}=T_4+\frac{(S-R)}{2.3C_H}. \tag{10}$$

The results show that the values of the ground surface temperature in Experiment 3 are much smaller than those obtained in the control experiment. At some grid points, the decrease of surface temperature is as much as 20°C. Fig. 10 shows a comparison of ground temperature (at two selected locations) between Experiment 3 and the control experiment. It can be seen that the maximum decreased and the minimum increased appreciably. This is reflected in smaller values (not shown) for diurnal oscillations obtained in Experiment 3.

Thus Experiment 3 gives a much more improved distribution of ground surface temperature *vis-à-vis* the control experiment. However, the approximations for G and LE [Eq. (9)] are not quite realistic. For example, the first condition $(G=0.3H)$ implies that the two processes (G and H) are exactly in phase and have the same constant ratio. This is at variance with observations. Moreover, the value of 0.3 for this ratio is not universal; in fact Sasamori estimated this value for dry soil only. Again the assumption of a Bowen ratio of unity is also not realistic, because observations (Brooks and Goddard, 1966) have shown that it has a significant

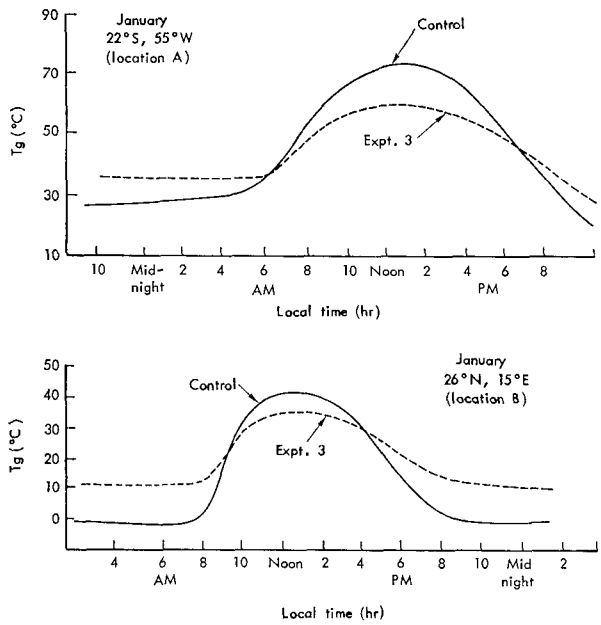

FIG. 10. As in Fig. 9 except for Experiment 3.

diurnal variation and sometimes changes sign also. It may be mentioned that Kasahara and Washington (1971) suggest a calibration of nighttime surface temperatures by controlling the ground temperature.

5. Prognostic equation for T_g: Experiment 4

Recently some GCM's (Corby *et al.*, 1972) have computed T_g for land points by solving a prediction equation:

$$c'\frac{\partial T_g}{\partial t}=S-R-LE-H, \tag{11}$$

where c' is the thermal capacity per unit lateral area of the surface layer; S, R, H and LE have the same meaning as in the control and other experiments. Eq. (11) is based on the assumption that there is no heat conduction from below and consequently T_g [given by Eq. (11)] represents the bulk temperature of the soil layer of finite depth and not the ground surface temperature. It is also evident that Eq. (11) cannot reproduce diurnal variation of surface temperature realistically.

In this section we describe a method which incorporates soil heat flux in Eq. (11) and with a suitable approximation can be used to compute the ground surface temperature T_g.

If we consider a soil layer from surface ($z=0$) to a depth z, then the time rate of temperature change for this layer is given by

$$c\frac{\partial T_s(z,t)}{\partial t}=-\left[\frac{G(z,t)-G(0,t)}{z}\right], \tag{12}$$

where c is the volumetric heat capacity (J m^{-3} K^{-1}), and $T_s(z,t)$ is the average temperature of the soil layer of depth z.

Also $G(0,t)\equiv S-R-LE-H$ represents the heat flux at the surface and [as shown in the Appendix, Eq. (A6)]

$$G(z,t)=\left(\frac{\omega c\lambda}{2}\right)^{\frac{1}{2}}\left[\frac{1}{\omega}\frac{\partial T_s(z,t)}{\partial t}+T_s(z,t)-\bar{T}\right] \tag{13}$$

represents the soil heat flux at depth z.

Since the main purpose of our study was to compute the ground surface temperature rather than "bulk" temperature of a soil layer of finite depth, we applied Eq. (12) to a soil layer of 1 cm depth and assumed that the average temperature for this layer approximates the ground surface temperature T_g. Thus

$$T_s(1,t)\approx T_g(t). \tag{14}$$

We believe that considering the uncertainty in defining "surface proper," particularly on global scale and also the crude horizontal resolution of our GCM (4° latitude, 5° longitude), Eq. (14) represents a reasonable approximation for our purposes. Thus using (14) in Eqs. (12) and (13) applied at $z=0.01$ m, we get (omitting t from parentheses)

$$c\frac{\partial T_g}{\partial t}=G(0)-\left(\frac{\omega c\lambda}{2}\right)^{\frac{1}{2}}\left[\frac{1}{\omega}\frac{\partial T_g}{\partial t}+T_g-\bar{T}\right],$$

or rearranging and inserting the expression for $G(0)$,

$$c_1\frac{\partial T_g}{\partial t}=S-R-LE-H-\left(\frac{\lambda c\omega}{2}\right)^{\frac{1}{2}}(T_g-\bar{T}), \tag{15}$$

where $c_1=c+(\lambda c/2\omega)^{\frac{1}{2}}$.

It may be noted that all terms on the right-hand side of Eq. (15), except S, are functions of T_g. Thus

$$c_1\frac{\partial T_g}{\partial t}=F(T_g), \tag{16}$$

where

$$F(T_g)\equiv S-R-LE-H-\left(\frac{\lambda c\omega}{2}\right)^{\frac{1}{2}}(T_g-\bar{T}).$$

Applying the backward implicit scheme to Eq. (16), and approximating

$$F(T_g^{t+\Delta t})=F(T_g^t)+\left[\frac{\partial F}{\partial T_g}\right]_{T_g^t}(T_g^{t+\Delta t}-T_g^t)$$

and solving for $T_g^{t+\Delta t}$, we get

$$T_g^{t+\Delta t}=T_g+\frac{S-R-H-LE-\left(\frac{\lambda c\omega}{2}\right)^{\frac{1}{2}}(T_g-\bar{T})}{\frac{c_1}{\Delta t}+4\nu T_g^3+C_H\left(1+\frac{L}{C_p}\mathrm{GW}\frac{dq_s}{dT}\right)+\left(\frac{\lambda c\omega}{2}\right)^{\frac{1}{2}}}. \tag{17}$$

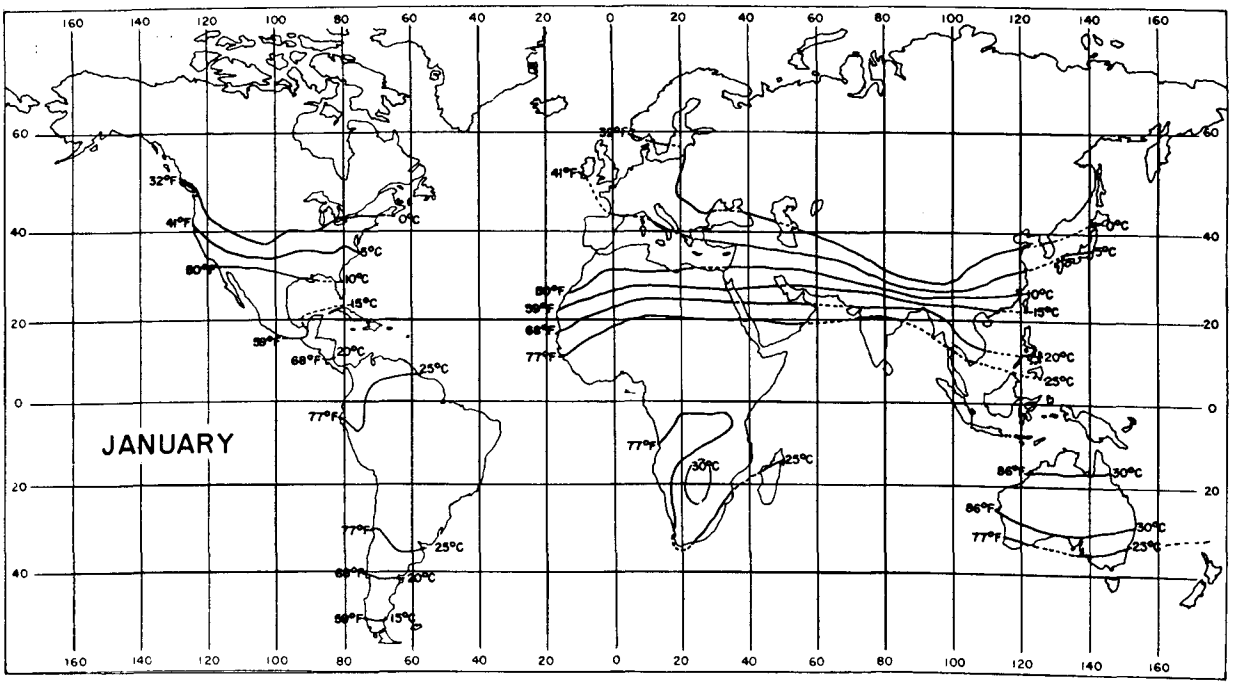

FIG. 11. Soil temperatures at 0.1 m depth—January (from Chang, 1958).

The superscript t has been omitted from the right side of Eq. (17). Thus, if the quantities on the right side are known at a given time t, then Eq. (17) can be used to predict T_g for future time $(t+\Delta t)$. Here $c_1=c+(\lambda c/2\omega)^{\frac{1}{2}}$ (c being the volumetric heat capacity), λ is the thermal conductivity (W m^{-1} K^{-1}), $\bar{T}$ the average daily surface temperature, assumed same at all depths (K), ω the frequency of oscillation (s^{-1}), Δt the time step for solving Eq. (17) [=30 min], and ν the Stefan-Boltzmann constant [=0.56 W m^{-2} K^{-4}].

In Eq. (18), we assign the same values for λ which were used in Experiments 1 to 3. For heat capacity c, which depends on moisture content and the nature of different soil constituents, we use a constant value of 2.5×10^6 J m^{-3} K^{-1} (Priestley, 1959; Geiger, 1965). An examination of Eq. (17) shows that the solution for T_g depends upon, among other factors, the value of $\bar{T}$, the average daily surface temperature. We tried two methods for estimating $\bar{T}$:

1) Computed $\bar{T}$ on the basis of the "past" day's values of T_g and used this average in computing T_g for the following day. This technique enabled us to let $\bar{T}$ vary on a daily basis; also it could be computed at each grid point.

2) Prescribed $\bar{T}$ as a function of latitude zones on the basis of observations. However, since there are no maps of soil temperature available on a daily basis, only monthly maps could be used. Consequently, solutions for T_g for any month on a daily basis were biased toward the value of $\bar{T}$ prescribed for that month.

We integrated the model for 48 h, using both the above techniques, and did not find any significant differences in the results, at least for the two days we considered. The results discussed in this paper are based on $\bar{T}$, which was prescribed as a function of latitude zones on the basis of a map of soil temperature at 0.1 m depth for January prepared by Chang (1958) (Fig. 11). The use of soil temperature at 0.1 m for $\bar{T}$ is justified because $\bar{T}$, by definition, is assumed to be independent of depth.

Fig. 12 shows the global distribution of daily maximum ground surface temperature obtained by solving Eq. (17). A comparison of these results with those of control experiment (Fig. 3) shows that there is in general considerable reduction in the amplitudes of maximum T_g and diurnal range. This is very significant in West Africa where the highest isotherm which for control experiment was 90°C, became 60°C in Experiment 4. The Sahara region, which was dominated by isotherms of 50°–60°C in control run was characterized by maximum temperatures of 30°–50°C. However, the results of Experiment 4 still show rather unrealistically high values for T_g in the equatorial forest region of Africa. This can be attributed to the absence of any precipitation and consequent evaporation, during the duration of model integration (48 hours) which is quite contrary to the real atmosphere situation. In fact, simulation of January climate by Gates (1972), using the Rand two-level GCM, has shown this region to be characterized by heavy precipitation. It can thus be expected that the unrealistically high values of T_g in

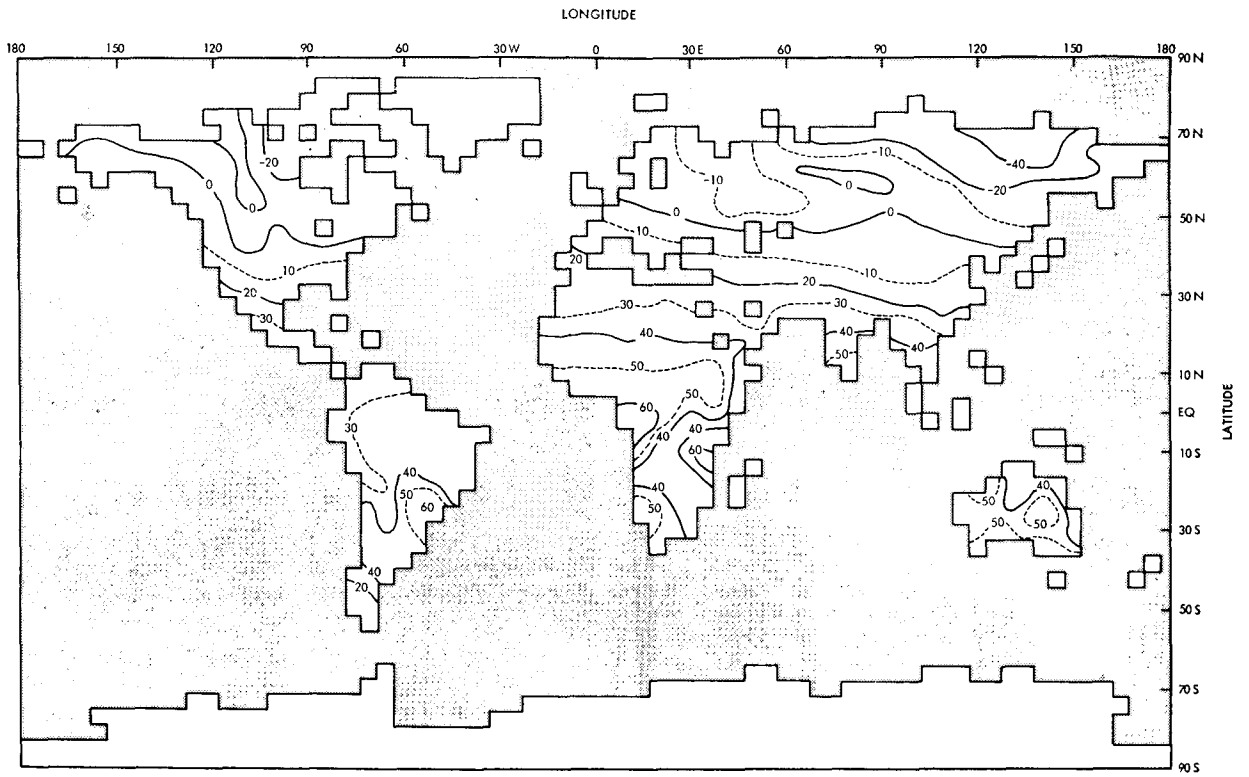

FIG. 12. Daily maximum ground surface temperature (°C): Experiment 4 (January).

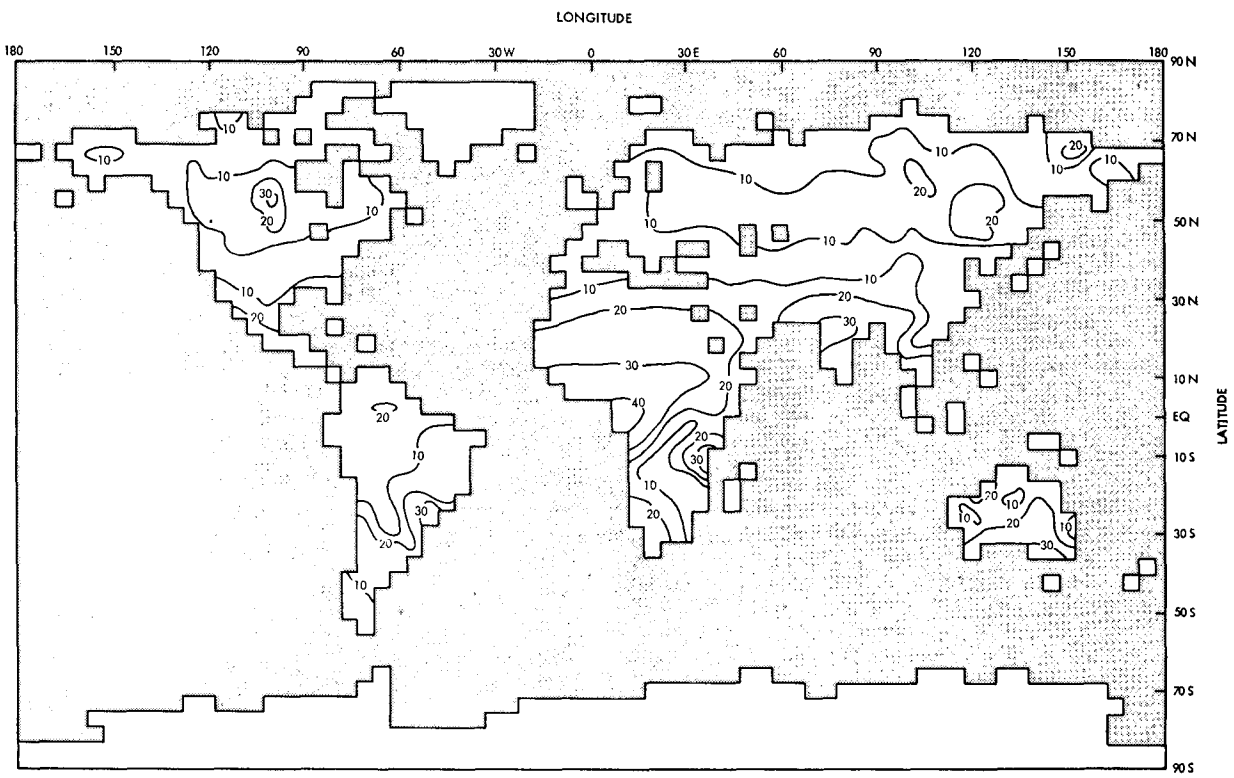

FIG. 13. Diurnal range of ground surface temperature (°C): Experiment 4 (January).

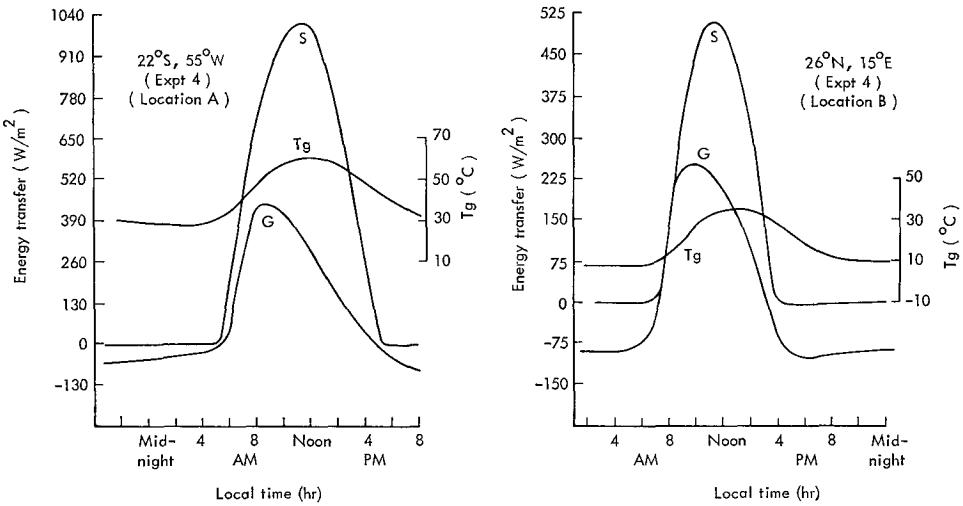

FIG. 14. As in Fig. 8 except for Experiment 4.

equatorial Africa will become realistic in any longterm integration of the model.

Fig. 13 shows the global distribution of diurnal range of T_g obtained in Experiment 4. Again the unrealistic features (values of 80° in West Africa) shown by control experiment (Fig. 4) have now become quite realistic, particularly in the summer hemisphere. The improvement of values in Australia and West Africa is quite significant; for example, there is a decrease of as much as 40°C in the value in West Africa and some parts of Australia. Fig. 14 shows plots of T_g, $G(0)$, S as a function of local time. It can be seen that while maximum G precedes maximum T_g by 3 h, maximum S does so by about 1 h. This phase relationship, produced by the interaction between various components of energy balance at the surface, agrees with observations (Johnson, 1954; Sellers, 1965) as well as with analytical solutions of the heat conduction equation.

6. Concluding remarks

We have integrated the Rand two-level atmospheric general circulation model to compute the ground surface temperature T_g (for bare land grid points) by incorporating the soil heat flux in the interface energy balance equation (Experiments 1 through 3); we have also computed T_g by solving a prognostic equation (Experiment 4). A comparison of the results shows that the most realistic distribution of T_g with respect to the magnitude, the diurnal range, and the phase relationship between T_g, solar radiation and soil heat flux is given by the prognostic equation. It may be noted that the methods described in this paper may not be applicable to surfaces which are covered with ice and/or snow, especially if these change with time. In that case one may use Eq. (11) with the recognition that a bulk temperature will be obtained and it may not be realistic to use this for estimating radiation and sensible heat flux at the surface.

In recent times, considerable attention has been paid to the study of climatic changes and their impact on worldwide economic and social order. Though modeling of climatic variation is still in developing stages, general circulation models are being used increasingly to study shorter period variations. And recognizing the importance of feedback effects of variations of surface temperature on atmospheric processes, it is essential to be able to compute, among other things, a realistic distribution of ground surface temperature. The technique described in this paper can be useful in this computation.

Acknowledgments. This research was sponsored by the Defense Advanced Research Projects Agency (ARPA) under Contract DAHC15-73-C-0181.

The author wishes to thank E. S. Batten and M. E. Schlesinger for very useful discussions. David Pass was responsible for the numerical integration of various experiments.

APPENDIX

An Expression for Heat Flux into the Soil

Assuming that soil is homogeneous and that heat flow is in the vertical direction only, the heat conduction equation can be written as

$$\frac{\partial T_s}{\partial t} = \frac{\lambda}{c}\frac{\partial^2 T_s}{\partial z^2}, \tag{A1}$$

where T_s is soil temperature, λ the thermal conductivity, and c the volumetric heat capacity. If we now assume that the temperature at the surface can be written as

$$T_s(0,t) = \bar{T} + \Delta T_0 \sin(\omega t), \tag{A2}$$

where $\bar{T}$ is daily average temperature of the soil assumed to be the same at all depths, ΔT_0 the amplitude at the surface, and ω the frequency of oscillation equal

to $2\lambda/(\text{period of the wave})$, then the solution of (A1) may be written as

$$T_s(z,t)=\bar{T}+\Delta T_0 e^{-z/d}[\sin(\omega t-z/d)], \qquad \text{(A3)}$$

where $T_s(z,t)$ is the soil temperature at the depth z and time t and $d=(2\lambda/c\omega)^{\frac{1}{2}}$ is the depth at which the amplitude of ΔT_0 is insignificant.

Again, for an infinitesimally thin soil layer, the heat flux into the soil is given by

$$G(z,t)=-\lambda\frac{\partial T_s}{\partial z}. \qquad \text{(A4)}$$

Combining (A3) and (A4), we obtain

$$G(z,t)=\Delta T_0\left(\frac{\omega c\lambda}{2}\right)^{\frac{1}{2}} e^{-z/d}[\sin(\omega t-z/d)+\cos(\omega t-z/d)]. \qquad \text{(A5)}$$

Eliminating ΔT_0, which is rarely known accurately, from Eq. (A5) by using Eq. (A3) and its differentiated form with respect to t, we get

$$G(z,t)=\left(\frac{\omega c\lambda}{2}\right)^{\frac{1}{2}}\left[\frac{1}{\omega}\frac{\partial T_s(z,t)}{\partial t}+T_s(z,t)-\bar{T}\right]. \qquad \text{(A6)}$$

REFERENCES

Brooks, F. A., and W. B. Goddard, 1966: Observed four-component hourly energy balance. Final Report, University of California, Davis.

Chang, Jen-Hu, 1958: *Ground Temperature*, Vol. I. Blue Hill Meteorological Observatory, Harvard University, Milton, Mass., 300 pp.

Corby, G. A., A. Gilchrist and R. L. Newson, 1972: A general circulation model for the atmosphere suitable for long term integrations. *Quart. J. Roy. Meteor. Soc.*, **98**, 809–832.

de Vries, D. A., 1963: Thermal properties of soils. *Physics of Plant Environment*, W. R. Van Wijk, Ed., New York, John Wiley & Sons, Inc., 210–235.

Delsol, F., K. Miyakoda and R. H. Clark, 1971: Parameterized processes in the surface boundary layer of an atmospheric circulation model. *Quart. J. Roy. Meteor. Soc.*, **97**, 181–208.

Estoque, M. A., 1963: A numerical model of the atmospheric boundary layer. *J. Geophys. Res.*, **68**, 1103–1113.

Gadd, A. J., and J. F. Keers, 1970: Surface exchanges of sensible and latent heat in a 10-level model atmosphere. *Quart. J. Roy. Meteor. Soc.*, **96**, 297–308.

Gates, W. L., 1972: The January global climate simulated by the two-level Mintz-Arakawa model: A comparison with observation. The Rand Corporation, R-1005-ARPA, 107 pp.

——, E. S. Batten, A. B. Kahle and A. B. Nelson, 1971: A documentation of the Mintz-Arakawa two-level atmospheric general circulation model. The Rand Corporation, R-877-ARPA, 408 pp.

Geiger, R., 1965: *The Climate Near the Ground*. Cambridge, Harvard University Press, 611 pp.

Jacobs, C. A., and P. S. Brown, Jr., 1973: An investigation of the numerical properties of the surface heat balance. *J. Appl. Meteor.*, **12**, 1069–1072.

Johnson, J. C., 1954: *Physical Meteorology*. Cambridge, The M.I.T. Press, 393 pp.

Kasahara, A., and W. Washington, 1971: General circulation experiments with a six-layer NCAR model, including orography, cloudiness and surface temperature calculations. *J. Atmos. Sci.*, **28**, 657–701.

Lonnquist, O., 1962: On the diurnal variation of surface temperature. *Tellus*, **14**, 96–101.

Manabe, S., J. Smagorinsky and R. F. Strickler, 1965: Simulated climatology of a general circulation model with a hydrologic cycle. *Mon. Wea. Rev.*, **93**, 769–798.

Myrup, L. O., 1969: A numerical model of the urban heat islands. *J. Appl. Meteor.*, **8**, 908–918.

Outcalt, S. I., 1972: The development and application of a simple digital surface-climate simulator. *J. Appl. Meteor.*, **11**, 629–636.

Pandolfo, J. P., D. S. Cooley and M. A. Atwater, 1965: The development of a numerical prediction model for the planetary boundary layer. Final Report, The Travelers Research Center, Inc., Hartford, Conn., 88 pp.

Priestley, C. H. B., 1959: *Turbulent Transfer in Lower Atmosphere*. The University of Chicago Press, 130 pp.

Sasamori, T., 1970: A numerical study of atmospheric and soil boundary layers. *J. Atmos. Sci.*, **27**, 1122–1137.

Sinclair, J. G., 1922: Temperatures of the soil and air in a desert. *Mon. Wea. Rev.*, **50**, 142–144.

Sellers, W. D., 1965: *Physical Climatology*. The University of Chicago Press, 272 pp.

Sutton, O., 1953: *Micrometeorology*. New York, McGraw-Hill, 333 pp.